

## A two-way nonreflecting wave equation

Edip Baysal\*, Dan D. Kosloff†, and J. W. C. Sherwood§

### ABSTRACT

In seismic modeling and in migration it is often desirable to use a wave equation (with varying velocity but constant density) which does not produce interlayer reverberations. The conventional approach has been to use a one-way wave equation which allows energy to propagate in one dominant direction only, typically this direction being either upward or downward (Claerbout, 1972).

We introduce a two-way wave equation which gives highly reduced reflection coefficients for transmission across material boundaries. For homogeneous regions of space, however, this wave equation becomes identical to the full acoustic wave equation. Possible applications of this wave equation for forward modeling and for migration are illustrated with simple models.

### INTRODUCTION

Forward modeling and migration often deal with symmetric wave propagation in which the raypath from the surface to the reflecting horizons is the same as the raypath from the reflecting horizons back to the surface. In such a situation it is often advantageous to model the propagation in only one direction along the raypath. In order to reproduce the arrival times correctly in such calculations, the material velocity must be halved with respect to the actual acoustic velocities in the medium (Lowenthal et al, 1976). It is also often desirable to eliminate multiple reflections and reverberations and produce synthetic sections which contain primary energy only. The common approach has been to use one-way equations which allow energy to propagate in one direction only (Claerbout, 1972; Gazdag, 1981). These equations do have their limitations and, in particular, they cannot simulate rays which turn around via refraction in the presence of large velocity gradients.

In this study we derive a two-way wave equation which simultaneously permits both upgoing and downgoing propagation. For homogeneous regions this wave equation becomes identical to the acoustic wave equation. However, in propagation from one medium to another this equation gives a zero reflection coefficient for normal incidence.

In the following sections we derive the two-way nonreflecting wave equation, and present examples which shed light on its features.

### DERIVATION OF THE TWO-WAY NONREFLECTING WAVE EQUATION

For a two-dimensional (2-D) medium with variable velocity  $C(x, z)$ , but with constant density, the acoustic wave equation is given by

$$\frac{\partial^2 P}{\partial x^2} + \frac{\partial^2 P}{\partial z^2} = \frac{1}{C^2(x, z)} \frac{\partial^2 P}{\partial t^2}, \quad (1)$$

where  $P$  denotes the pressure, and  $x$  and  $z$  are the Cartesian coordinates (Kosloff and Baysal, 1982). Consider next one-dimensional (1-D) wave propagation, say in the  $x$  direction, when the velocity  $C$  is constant. For this type of motion, equation (1) can be rewritten symbolically as

$$\left( C \frac{\partial}{\partial x} - \frac{\partial}{\partial t} \right) \left( C \frac{\partial}{\partial x} + \frac{\partial}{\partial t} \right) P = 0. \quad (2)$$

If only the first bracketed term in equation (2) is retained, we obtain a one-way wave equation given by

$$C \frac{\partial P}{\partial x} - \frac{\partial P}{\partial t} = 0. \quad (3)$$

The solutions to equation (3) are given by  $P = f(x + Ct)$  with  $f$  an arbitrary function. This solution gives a wave propagating in the negative  $x$  direction. In the same manner the second bracketed term in equation (2) gives wave propagation in the positive  $x$  direction.

When the velocity  $C$  in equation (2) is allowed to vary, the following 1-D wave equation is obtained:

$$C \frac{\partial}{\partial x} \left( C \frac{\partial P}{\partial x} \right) = \frac{\partial^2 P}{\partial t^2}. \quad (4)$$

A generalization of equation (4) to two dimensions gives

$$C \frac{\partial}{\partial x} \left( C \frac{\partial P}{\partial x} \right) + C \frac{\partial}{\partial z} \left( C \frac{\partial P}{\partial z} \right) = \frac{\partial^2 P}{\partial t^2}. \quad (5)$$

Equation (5) is the two-way nonreflecting wave equation. It

Manuscript received by the Editor September 7, 1982; revised manuscript received August 1, 1983.

\*Geophysical Development Corporation and Seismic Acoustics Lab of the University of Houston.

†Geophysics Department, Tel-Aviv University, Tel-Aviv, Israel, and Seismic Acoustics Lab of the University of Houston.

§Geophysical Development Corporation, 8401 Westheimer, Houston, TX 77063.

© 1984 Society of Exploration Geophysicists. All rights reserved.

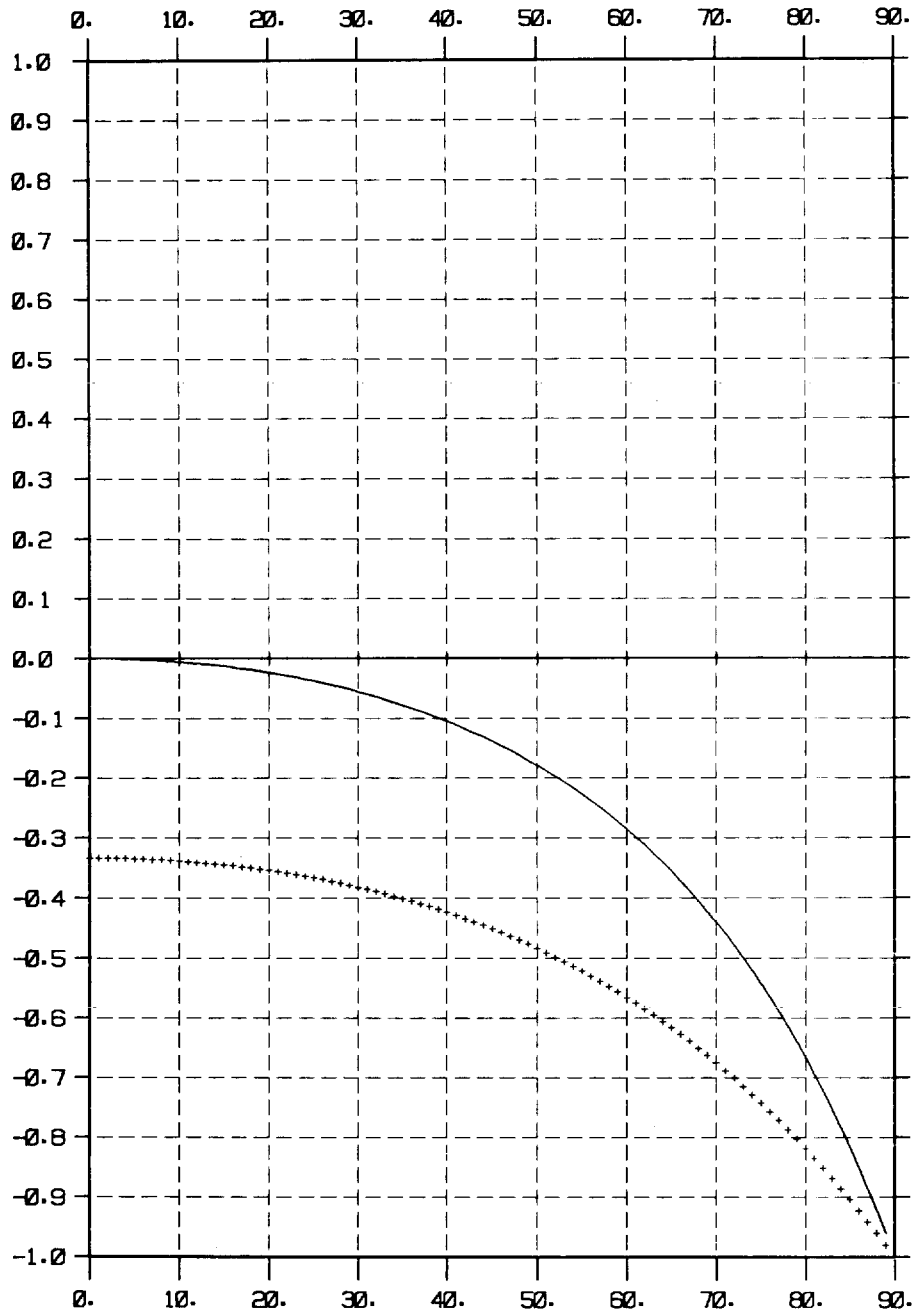


FIG. 1. Reflection coefficient as a function of incident angle for the case  $C_1 = 2C_2$ . + = acoustic wave equation. - = nonreflecting wave equation.

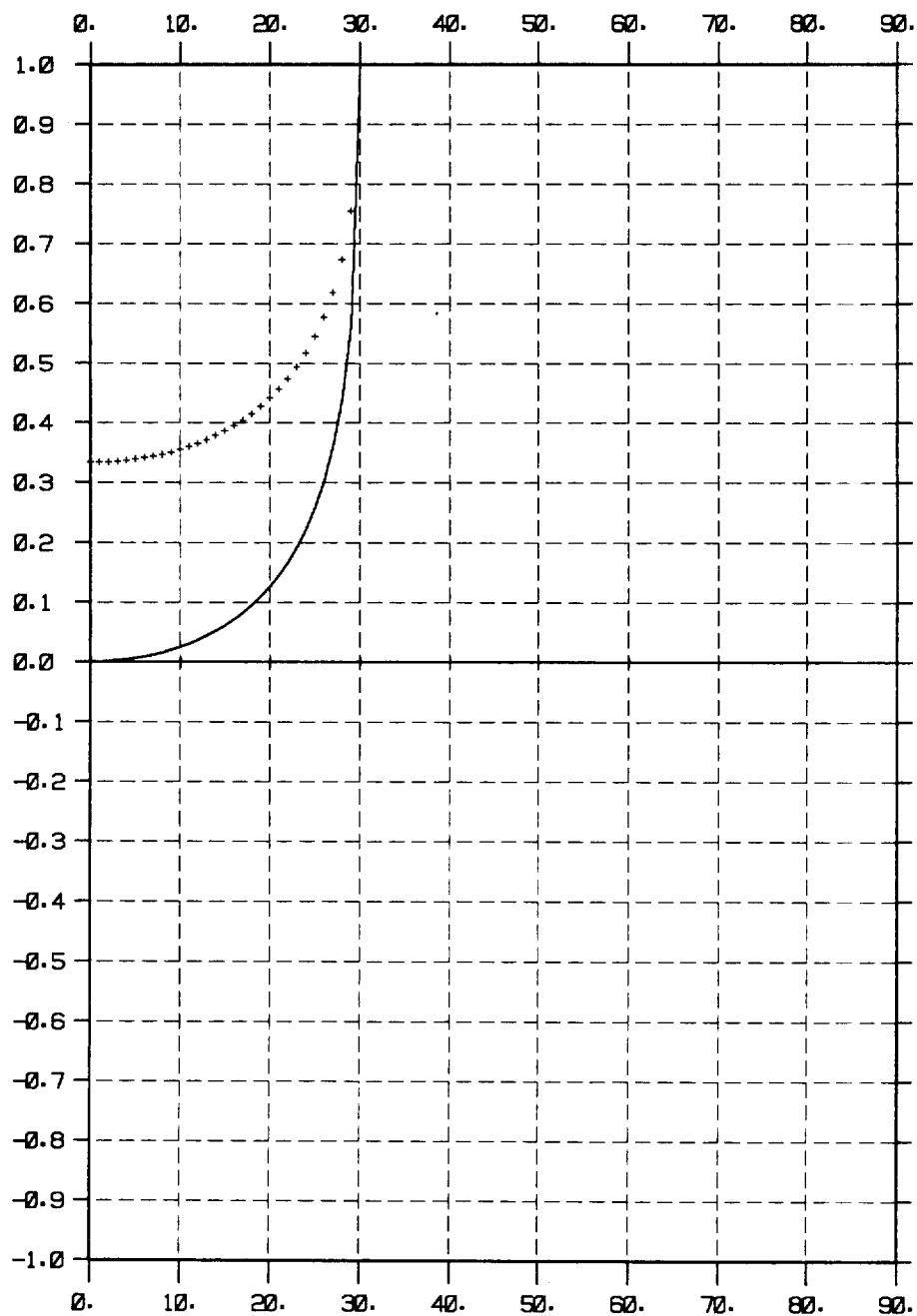


FIG. 2. Reflection coefficient as a function of incident angle for the case  $C_1 = 0.5C_2$ . + = acoustic wave equation, - = nonreflecting wave equation.

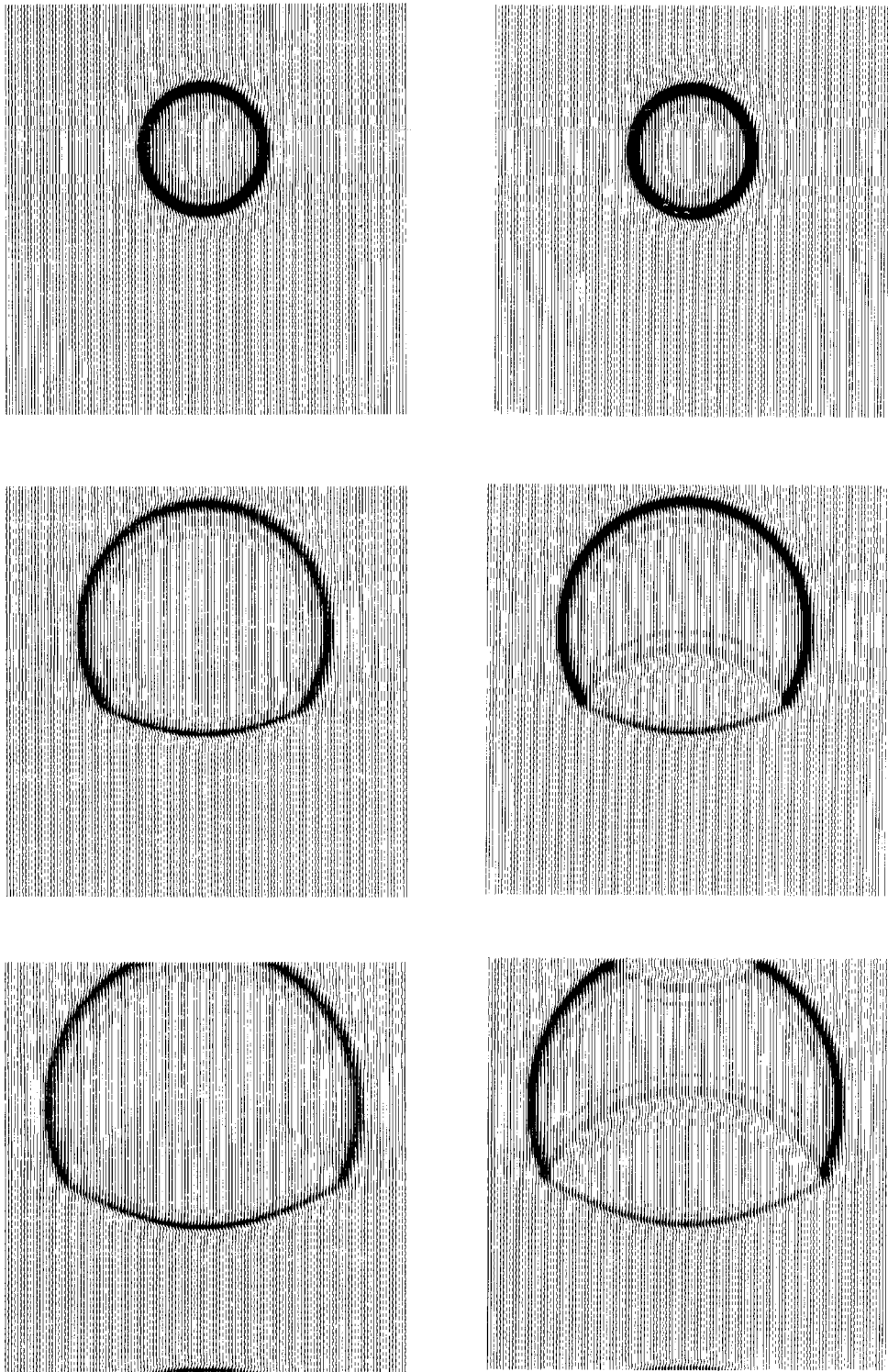


FIG. 3. Wavefront display comparison between acoustic and nonreflecting wave equations for the plane layer case ( $C_1 = 2C_2$ ).

degenerates into the usual acoustic wave equation (1) whenever the velocity  $C$  is constant. However, this wave equation does not give reflection in the case of normal incidence on a plane boundary which separates two dissimilar media; hence the term “two-way nonreflecting wave equation.”

It is interesting to note that for the case of a plane boundary between two regions, equation (5) gives small reflection coefficients for a range of incidence angles. For example, Figure 1 presents the reflection coefficients as a function of angle for propagation from a region of high velocity into a region of low velocity, where the velocity ratio has been chosen as 2 : 1. As the figure shows, the reflection coefficients remain low for a wide range of incidence angles. The opposite case, where the propagation is from a low-velocity region into a high-velocity region, is shown in Figure 2. The incidence angles in this figure range between zero and critical. As the figure shows, the reflection coefficients remain low for small angles, but increase when

the critical angle is approached. The numerical results presented in the next section are consistent with the reflectivity characteristics depicted in Figures 1 and 2.

Equation (5) can also be regarded as the full acoustic wave equation for a medium with constant impedance. The full equation, with the density  $\rho$  and the velocity  $C$  given as functions of the spatial coordinates, can be written (Kosloff and Baysal, 1982)

$$\frac{\partial}{\partial x} \left[ \frac{1}{\rho} \frac{\partial P}{\partial x} \right] + \frac{\partial}{\partial z} \left[ \frac{1}{\rho} \frac{\partial P}{\partial z} \right] = \frac{1}{\rho C^2} \frac{\partial^2 P}{\partial t^2}. \quad (6)$$

Now let the impedance  $\rho C$  be constant so that

$$\rho C = K \quad (7)$$

and use equation (7) to eliminate  $\rho$  from equation (6). The result is equation (5).

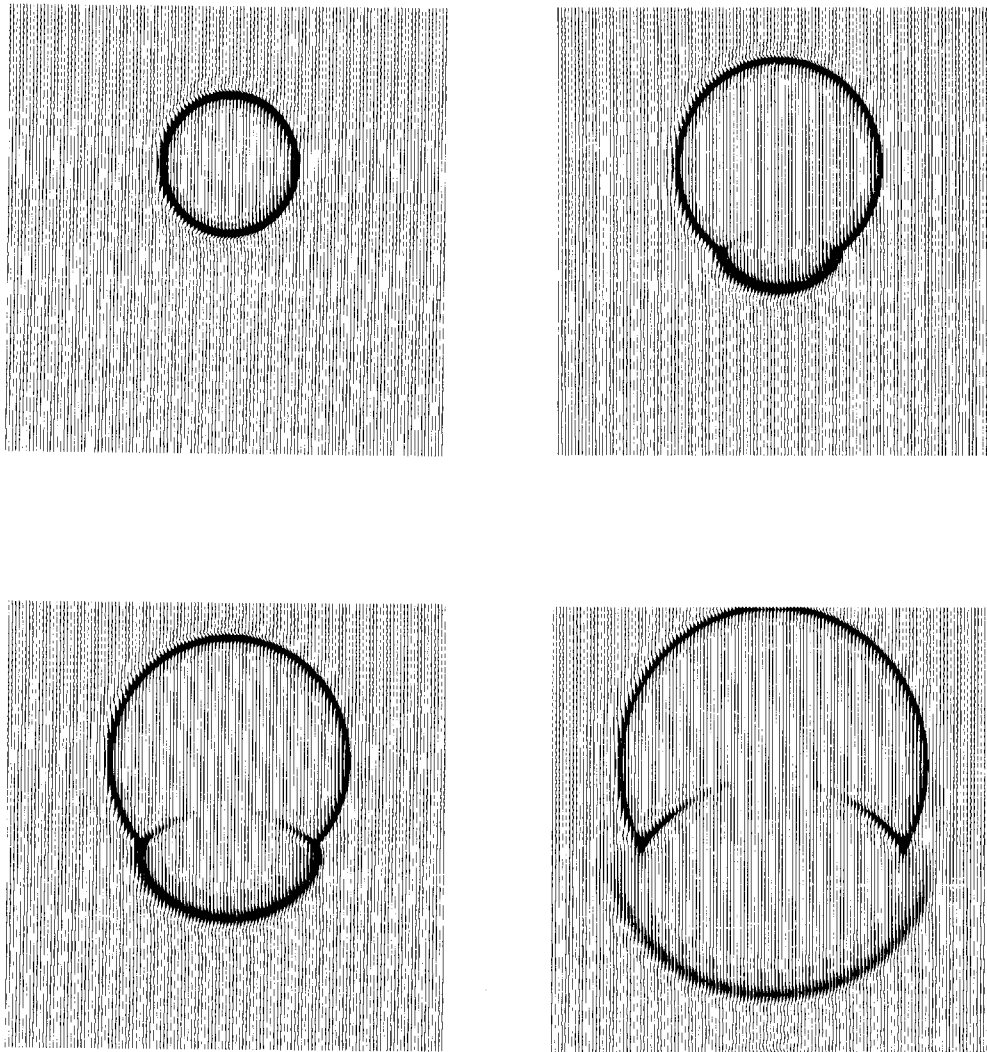


FIG. 4. Wavefront displays of nonreflecting wave equation for plane layer case ( $C_1 = 0.5C_2$ ).

Since equation (5) describes wave propagation in a medium in which the impedance remains constant, a wave that crosses an interface at normal incidence will have a zero reflection coefficient. In general, if the angle of incidence is  $\theta_1$  and the angle of refraction is  $\theta_2$ , then the reflection coefficient is given by

$$R = \left[ \frac{\rho_2 C_2 / \cos \theta_2 - \rho_1 C_1 / \cos \theta_1}{\rho_2 C_2 / \cos \theta_2 + \rho_1 C_1 / \cos \theta_1} \right], \quad (8)$$

(Aki and Richards, 1980). When the impedance is constant  $\rho_2 C_2 = \rho_1 C_1$  and the equation (8) reduces to

$$R = \frac{\cos \theta_1 - \cos \theta_2}{\cos \theta_1 + \cos \theta_2}. \quad (9)$$

#### EXAMPLES

In the first example the nonreflecting wave equation is compared with the full acoustic wave equation. The model consists

of two materials with a velocity ratio of 2 : 1. A point source is located in the high-velocity medium 960 ft above the plane interface separating the two media. A grid size of 128 by 128 was used in the computations where the grid spacing in both directions  $x$  and  $z$  was 40 ft. Amplitude values as a function of space for three different times are displayed in Figure 3. The "frozen time" sections on the left-hand side of Figure 3 were obtained with the nonreflecting wave equation, whereas those on the right side resulted from the full acoustic wave equation. The comparison clearly shows that the nonreflecting wave equation reduces the amplitudes of the reflected wave to almost zero and that the transmitted wavefront remains undistorted. The results are in qualitative agreement with Figure 1.

In the second example the model is reversed. The upper medium is the low-velocity medium, where the velocity ratio between the two media is still 1 : 2. The wavefront displays for four different times are presented in Figure 4. The amplitude of the reflected wave changes with the incident angle as Figure 2 suggests. Reflection is greatly reduced for incident angles sub-

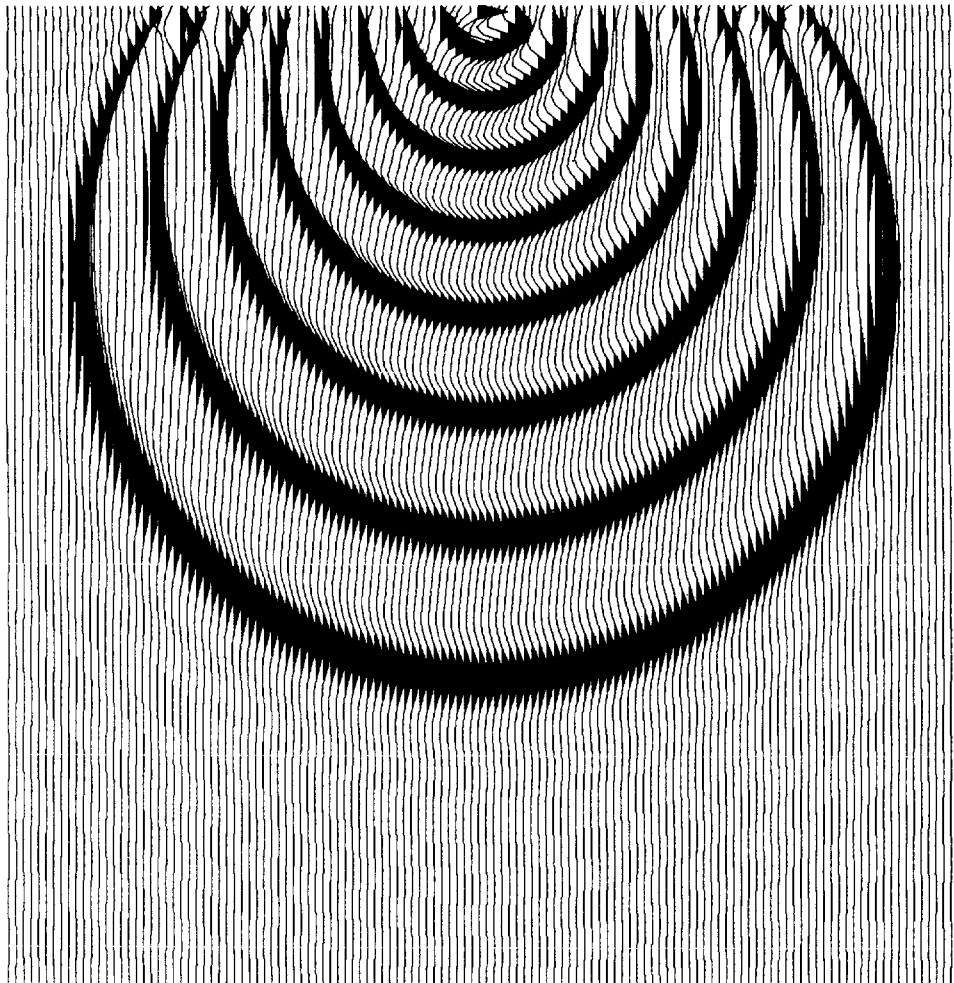


FIG. 5. Superimposed wavefronts for linearly increasing velocity medium.

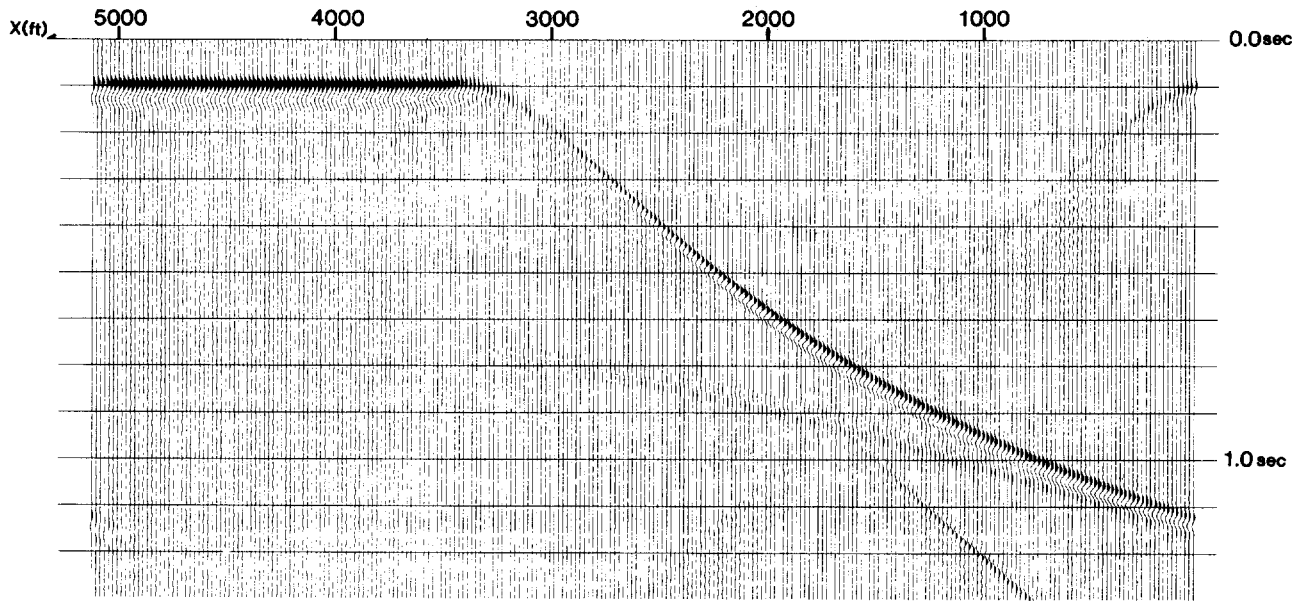
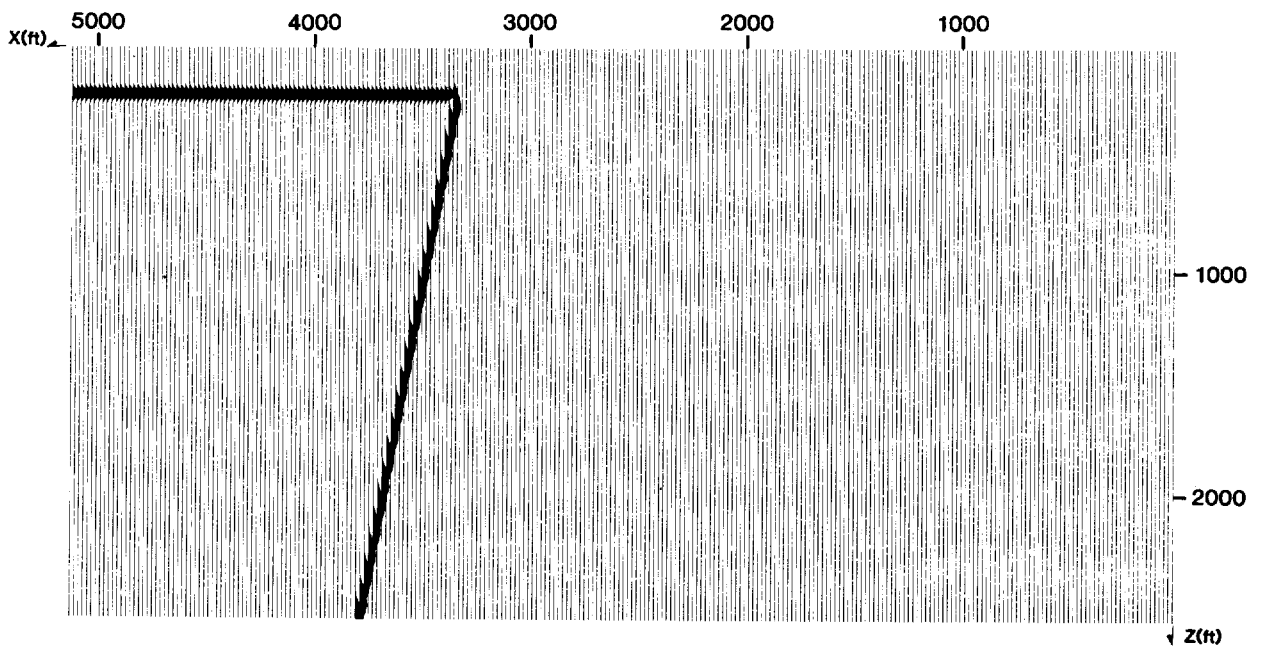


FIG. 6. Time section over the fault block model.

FIG. 7. Wavefront display of the fault block model for  $t = 0.0$  sec.

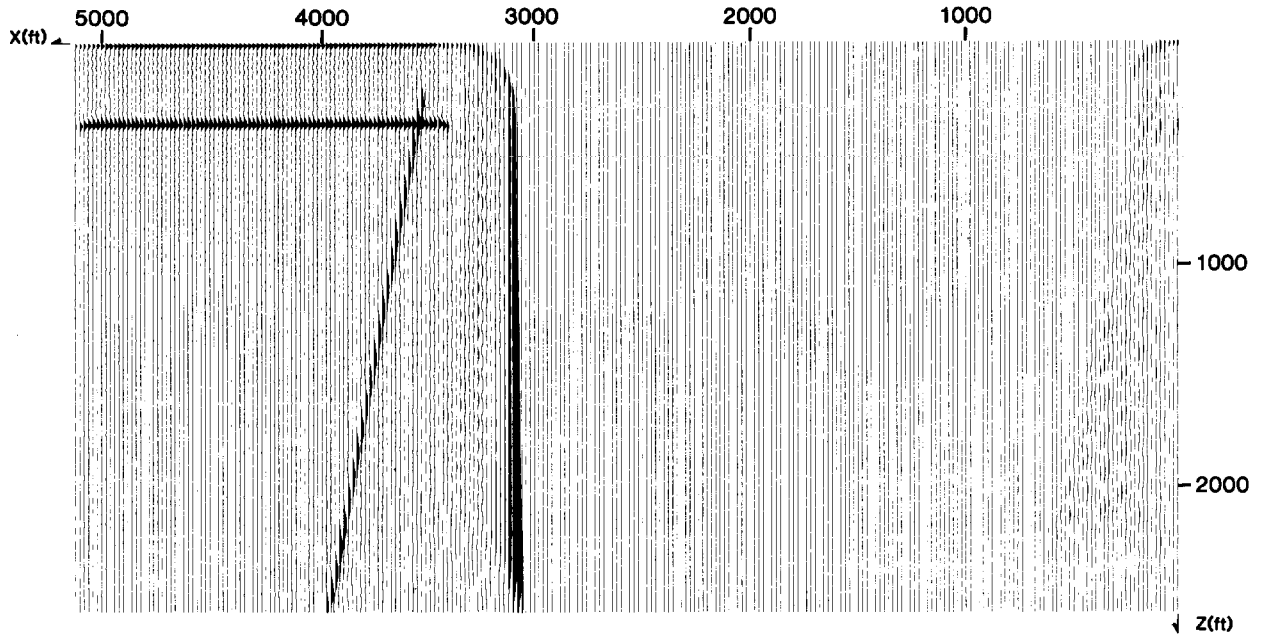


FIG. 8. Wavefront display of the fault block model for  $t = 0.1$  sec.

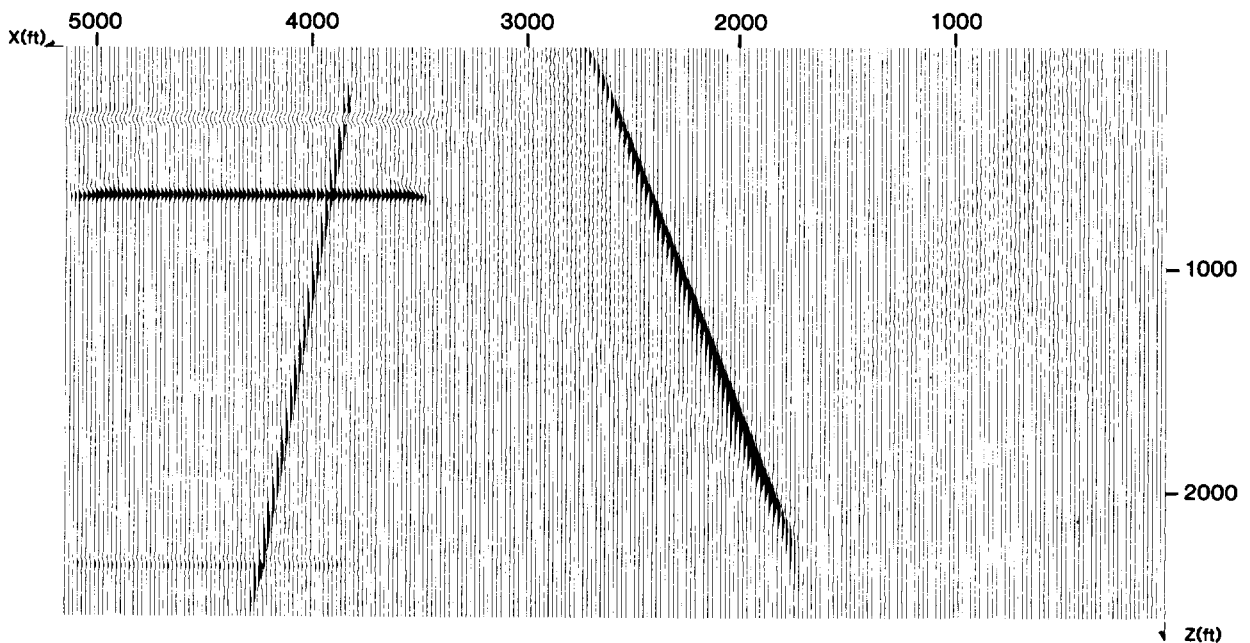


FIG. 9. Wavefront display of the fault block model for  $t = 0.3$  sec.



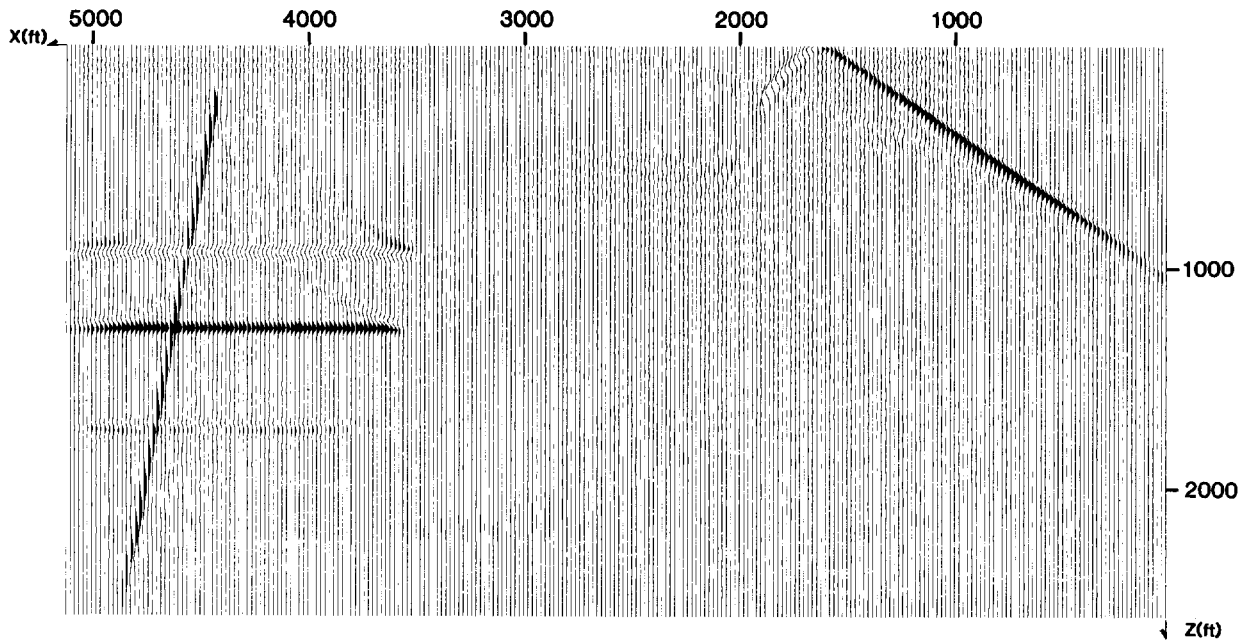


FIG. 10. Wavefront display of the fault block model for  $t = 0.7$  sec.

stantially smaller than the critical angle. Because of the extreme velocity ratio of 1:2, the critical angle is rather small (30 degrees).

The next example is a point source in a medium with a linear increase in velocity. In order to see the effect of the velocity gradient, the wavefront displays for increasing values of time are superimposed in Figure 5. Theoretically the wavefronts should be circular, with the center of the circles moving vertically downward in space as traveltimes advances (Slotnick, 1959). The results in Figure 5 are completely consistent with the theoretical expectations.

Finally, a zero source-receiver offset seismic section is simulated over a structural model using the "exploding reflector" concept introduced by Loewenthal et al (1976). The model consists of a fault block with a constant velocity of 3000 ft/sec, the fault plane having a steep dip of 80 degrees (see Figure 7). The medium to the right of the fault block has a large vertical velocity gradient. The velocity of this medium starts with 4000 ft/sec at the surface and increases linearly with depth with a gradient of 4 ft/sec per foot. If a one-way equation is used in the modeling, then it is impossible to simulate the surface arrival due to the wavefront generated at the fault plane, which starts traveling downward, then turns around via refraction due to the velocity gradient, and arrives at the surface stations that are not located directly above the fault block. It is possible to model these raypaths with equation (1), but this will also generate events such as reverberations or multiples between the horizontal upper boundary of the fault block and the free surface. The nonreflecting wave equation [equation (5)] will correctly model the raypaths which turn around because of the velocity gradient and then arrive at the surface, whereas it also will greatly reduce the amplitudes of the undesirable secondary

events. Figure 6 presents the resulting seismic section over this model using the nonreflecting wave equation. The reflections from the horizontal upper boundary of the fault block and the reflections from the fault plane by curved raypaths are connected by the diffractions caused by the corner of the fault block.

The next set of figures shows the amplitude displays as a function of space at different times. Figure 7 is at time  $t = 0$  sec and therefore it represents the initial pressure field (in this model the sources located at the material interfaces were assigned a strength of unity). Figures 8, 9, and 10 are the wavefront displays at corresponding times of  $t = 0.1, 0.3, 0.7$  sec. It is possible to observe the change of direction of the wavefront which started at the fault plane. It starts out traveling downward; in Figure 8 the wavefront is turned around and is almost vertical, then it continues to turn around and travels upward in Figures 9 and 10. The fault plane also emits another wave which travels slightly upward in the low-velocity fault block, and it hits the upper horizontal boundary of the fault block with an incident angle larger than the critical angle. Therefore no transmission occurs at this interface, and the surface stations above the fault block cannot record anything caused by the fault plane (Figure 7). The waves associated with the upper horizontal boundary of the fault block provide some interesting features. This boundary emits both an upward and a downward traveling wave. The upward traveling wave arrives at the surface (Figure 8) where it is reflected back by the free surface (Kosloff and Baysal, 1982). In Figures 9 and 10 the original downgoing wave emitted by the horizontal boundary of the fault block and the free-surface reflected wave following it with reverse polarity are obvious. Note that the reflections from the upper boundary of the fault block are eliminated due to the use of the nonreflecting wave equation.

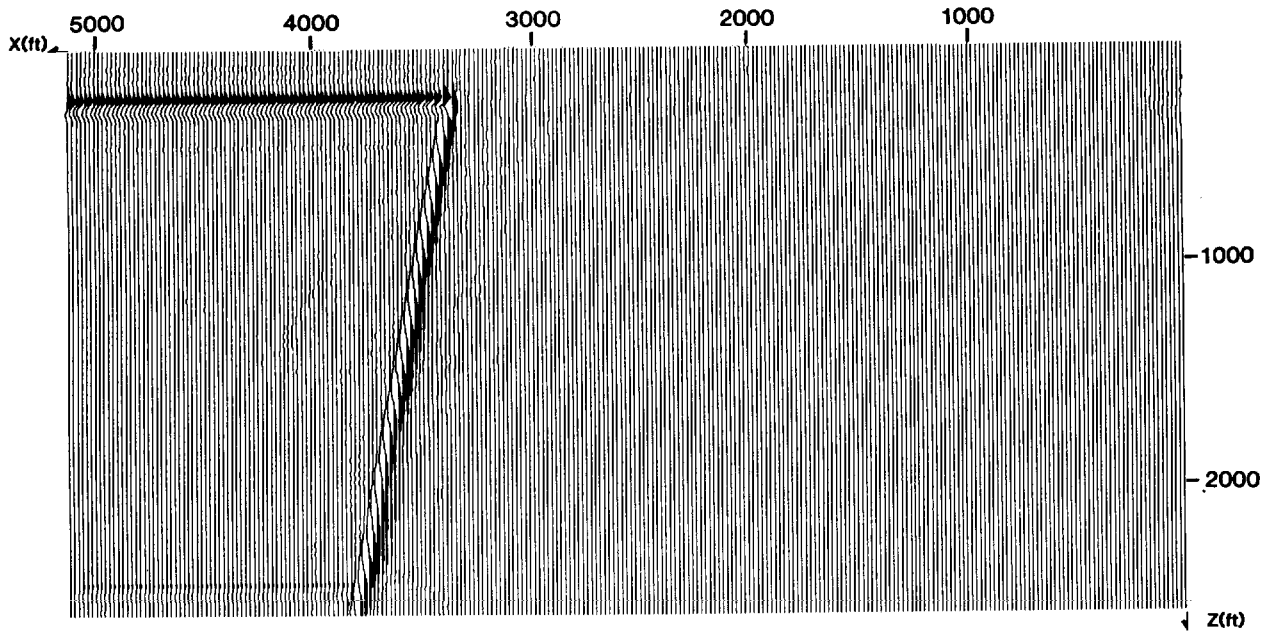


FIG. 11. Migrated depth section for the time section shown in Figure 6, using the nonreflecting wave equation and reverse time migration.

#### “REVERSE TIME” DEPTH MIGRATION USING THE NONREFLECTING WAVE EQUATION

Because multiple reflections are suppressed when multifold data are stacked, it seems appropriate to migrate a stacked section using an equation which does not generate multiples. One-way wave equations have been used for this purpose, and they work well provided the wavefronts we wish to follow do not exceed appropriate steep dip limitations. Using the nonreflecting wave equation in place of the one-way wave equation avoids this restriction and at the same time retains the advantage of suppressing multiples.

The example of depth migration given here illustrates the ability of the nonreflecting wave equation to migrate a stacked section when the velocity distribution has a large vertical gradient. The synthetic time section shown in Figure 6 was used for the demonstration.

The imaging principle inherent in the migration of stacked sections permits a different approach to migration based on reverse time marching instead of depth extrapolation. The stacked section is considered as a surface boundary condition for a reverse operation to the modeling type wave calculations that step forward in time. Commencing with zeroes for the spatial pressure field and its time derivative, the calculations are carried out in reversed time from the time of the last sample on the time section until time zero when the amplitudes in all space are considered as the final migrated section. If the velocities for the migration are chosen correctly, the wave field at time zero should be coincident with the reflecting horizons in the medium.

The result of applying this algorithm to the data shown in Figure 6 is the depth section shown in Figure 11. The overhanging fault block has imaged, the success of the method being tied

to our knowledge of the velocity distribution.

#### CONCLUSIONS

We have presented a two-way wave equation which significantly reduces reflections from material interfaces. This equation can be useful in forward modeling or reverse-time depth migration when there is a need to avoid interlayer reverberations. It offers improvements over modeling or migration with one-way equations for structures with strong velocity contrasts or gradients where geometrical rays can turn around. In such situations, the two-way nonreflecting wave equation can follow the ray beyond the turning point.

#### ACKNOWLEDGMENT

The authors wish to express their appreciation to G. H. F. Gardner, Editor of *GEOPHYSICS*, for his patience and generous contributions of time and technical content during the final preparation of this article.

#### REFERENCES

- Aki, K., and Richards, P., 1980, *Quantitative seismology: v. 1*, W. H. Freeman Co.
- Claerbout, J., and Doherty, S., 1972, Downward continuation of moveout corrected seismograms: *Geophysics*, v. 37, p. 741–768
- Gazdag, J., 1981, Modeling of the acoustic wave equation with transform methods: *Geophysics*, v. 46, p. 854–859
- Kosloff, D. D., and Baysal, E., 1982, Forward modeling by a Fourier method: *Geophysics*, v. 46, p. 854–859
- E., 1982, Forward modeling by a Fourier method: *Geophysics*, v. 47, p. 1402–1412
- Loewenthal, D., Lu, L., Roberson, R., and Sherwood, J. W. C., 1976, The wave equation applied to migration: *Geophys. Prosp.*, v. 24, p. 380–399
- Slotnick, M. M., 1959, *Lessons in seismic computing*: R. A. Geyer, Ed., SEG, Tulsa.